ISSN 1063-7834, Physics of the Solid State, 2017, Vol. 59, No. 10, pp. 1940–1946. © Pleiades Publishing, Ltd., 2017.
Original Russian Text © D.A. Balaev, S.I. Popkov, A.A. Krasikov, A.D. Balaev, A.A. Dubrovskiy, S.V. Stolyar, R.N. Yaroslavtsev, V.P. Ladygina, R.S. Iskhakov, 2017, published in Fizika Tverdogo Tela, 2017, Vol. 59, No. 10, pp. 1920–1926.

MAGNETISM

Temperature Behavior of the Antiferromagnetic Susceptibility of Nanoferrihydrite from the Measurements of the Magnetization Curves in Fields of up to 250 kOe

D. A. Balaev[a, b, *], S. I. Popkov[a, b], A. A. Krasikov[a, b], A. D. Balaev[a], A. A. Dubrovskiy[a], S. V. Stolyar[a, b], R. N. Yaroslavtsev[a, b], V. P. Ladygina[c], and R. S. Iskhakov[a]

[a] *Kirensky Institute of Physics, Siberian Branch, Russian Academy of Sciences, Akademgorodok 50, Krasnoyarsk, 660036 Russia*

[b] *Siberian Federal University, Svobodnyi pr. 79, Krasnoyarsk, 660041 Russia*

[c] *Presidium of the Federal Scientific Center "Krasnoyarsk Scientific Center," Siberian Branch, Russian Academy of Sciences, Akademgorodok 50, Krasnoyarsk, 660036 Russia*

**e-mail: dabalaev@iph.krasn.ru*

Received April 4, 2017

Abstract—The cross-breeding problem of the temperature dependence of the antiferromagnetic susceptibility of ferrihydrite nanoparticles is considered. Iron ions Fe^{3+} in ferrihydrite are ordered antiferromagnetically; however, the existence of defects on the surface and in the bulk of nanoparticles induces a noncompensated magnetic moment that leads to a typical superparamagnetic behavior of ensemble of the nanoparticles with a characteristic blocking temperature. In an unblocked state, magnetization curves of such objects are described as a superposition of the Langevin function and the linear-in-field contribution of the antiferromagnetic "core" of the nanoparticles. According to many studies of the magnetization curves performed on ferrihydrite (and related ferritin) nanoparticles in fields to 60 kOe, dependence $\chi_{AF}(T)$ decreases as temperature increases, which was related before to the superantiferromagnetism effect. As the magnetic field range increases to 250 kOe, the values of χ_{AF} obtained from an analysis of the magnetization curves become lower in magnitude; however, the character of the temperature evolution of χ_{AF} is changed: now, dependence $\chi_{AF}(T)$ is an increasing function. The latter is typical for a system of AF particles with random orientation of the crystallographic axes. To correctly determine the antiferromagnetic susceptibility of AF nanoparticles (at least, ferrihydrite) and to search for effects related to the superantiferromagnetism effect, it is necessary to use in experiments the range of magnetic field significantly higher than that the standard value 60 kOe used in most experiments. The study of the temperature evolution of the magnetization curves shows that the observed crossover is due to the existence of small magnetic moments in the samples.

DOI: 10.1134/S1063783417100031

1. INTRODUCTION

Despite a great quantity of works on studying magnetic nanoparticles, many observed properties of such objects remain unexplained up to now, since the areas of their application in practice have expanded continuously. Among such problems is the description of the magnetization curve of nanosized particle of materials that exhibit antiferromagnetic (AF) order in bulk state [1–6]. In such nanoparticles, the AF order is conserved, as a rule, in the "core," but surface effects and defects lead to the appearance of a noncompensated magnetic moment of particles μ_P [6–11], and the existence of broken chemical bonds in the presence of AF interactions can be a reason of the spin-glass behavior of surface atoms [10–17].

At temperatures higher than the superparamagnetic (SP) blocking temperature T_B, the magnetization curve M(H) of AF particles is described by formula

$$M(H) = M_0 L(\mu_P, H) + \chi_{AF} H. \quad (1)$$

The first term in Eq. (1) corresponds to processes of the alignment of noncompensated magnetic moments along the direction of an external magnetic field, which are described by the classical Langevin function $L(\mu_P H) = \coth(\mu_P, H/kT) - 1/(\mu_P, H/kT)$ (M_0 is the saturation magnetization). The second term in Eq. (1) describes the sublattice angularity of an AF "core" of particles in the external field; χ_{AF} is the AF susceptibility.

In many cases, the correct description of the experimental dependences M(H) of AF particles requires the inclusion of the particle magnetic moment distri-

bution function [8, 15–19]. In this case, Eq. (1) can be rewritten as

$$M(H) = N_P \int_{\mu_{min}}^{\mu_{max}} L(\mu_P, H) f(\mu_P) \mu_p d\mu_P + \chi_{AF} H. \quad (2)$$

Here, N_P is the number of particles in a mass unit of a sample, and $f(\mu_P)$ is the particle magnetic moment distribution function. The description of the experimental data using Eqs. (1) and (2) allows to obtain the value of the mean magnetic moment of particles $\langle \mu_P \rangle$, values of χ_{AF}, and also their temperature evolution. In most cases, it turned out that temperature dependence $\chi_{AF}(T)$ of the antiferromagnetically ordered ferrihydrite (and also ferritin) that is studied in this work was a function decreasing as temperature increased [8, 15, 18–27], which profoundly contradicted the standard behavior of the antiferromagnetic susceptibility of a bulk antiferromagnet with a random orientation of the crystallographic axes at temperatures lower than the Néel temperature χ_{AF} (as in the case of a polycrystal, where χ_{AF} increases with temperature). The observed "anomalous" behavior of dependence $\chi_{AF}(T)$ in the nanoparticles has frequently been explained by the influence of the superantiferromagnetism effect.

This effect was predicted by Néel [28, 29] and implied that the surface spins in the AF particles with an even number of ferromagnetic planes were rotated under action of an applied field (**H** was perpendicular to the easy-magnetization axis) to a larger degree than spins of "internal planes." A noticeable increase in the AF susceptibility can be observed for the particles containing several dozen of ferromagnetically ordered planes in their diameters, which was the case in the particles studied in [8, 15, 18–27].

However, the majority of the studies of nanoparticles of ferrihydrite and ferritin were commonly performed in external magnetic fields not higher than ~60 kOe. In this range of fields, at temperatures higher ~100 K, dependence M(H) predicted by the Langevin function for magnetic moments of $10–30\mu_B$ (μ_B is the Bohr magneton) was close to a linear dependence. This circumstance contributed an ambiguity to the procedure of processing of the experimental magnetization curves M(H) using Eqs. (1) and (2) due to the same functional dependence for small particles (μ_P ~$10–30\mu_B$) and to "the response" of the AF ordered particle "core" (the second term of Eqs. (1), (2)). Therefore, to more correctly determine the values of χ_{AF} by Eqs. (1), (2), it is appropriate to expand the range of external magnetic fields upon experimental study of magnetization of the AF nanoparticles.

It was shown in [4] that the "anomalous" decrease in χ_{AF} with an increase in T observed in an AF ordered ferritin and observed from the processing of dependences M(H) in the range to 60 kOe can be a result of the influence of small magnetic moments of the nanoparticles or a magnetic anisotropy and cannot be related to the superantiferromagnetism effect.

In [30], it was shown that the results of analyzing dependence M(H) of a synthetic ferrihydrite (size of ~5.5 nm) using Eqs. (1) and (2) were dependent on the magnetic field range. The processing of the experimental data obtained in fields to 120 kOe gave slightly lower values of χ_{AF} than those for the range 40–60 kOe (at $T = 100$ K).

In this work, we studied the processes of high-field magnetization of ferrihydrite using the technique of pulsed magnetic fields to 250 kOe. We used the ferrihydrite (nominal formula $5Fe_2O_3 \cdot 9H_2O$) that was a bacterial activity product (so called bacterial ferrihydrite [31]). It was shown before that a low-temperature annealing of the initial sample led to a particle consolidation and, as a result, to an increase in their superparamagnetic blocking temperature T_B [32] and noncompensated magnetic moment μ_P [33], which made it possible to study the properties of ferrihydrite nanoparticles with different mean sizes [34, 35]. An analysis of the magnetization curves using Eq. (2) in the temperature range $T > T_B$ in the field range to 60 kOe showed that the dependence $\chi_{AF}(T)$ of the bacterial ferrihydrite was also a function decreasing as temperature increased. On the one hand, this agreed with the results of other studies of ferrihydrite (19, 21, 22, and 24–27] and ferritin [15, 18, 20, 23] (in ferritin, ferrihydrite particles are enclosed into a protein shell). On the other hand, to more correctly elucidate the behavior of $\chi_{AF}(T)$, it is necessary to study the magnetization curves in a wider range of magnetic fields [14]. We performed the measurements in the field range to 250 kOe on two bacterial ferrihydrite samples from the series that was studied in [33].

2. EXPERIMENTAL

2.1. Preparation and Characterization of Samples

The preparation of nanoferrihydrite formed as a result of activity of Klebsiella oxytoca bacteria was described in [6, 31]. The samples studied in this work were subjected to additional low-temperature annealing in air at 140°C for 3 and 240 h (further, they are denoted as 3h and 240h). According to the data of transmission electron microscopy and the values of the mean particle magnetic moment $\langle \mu_P \rangle$ obtained from the magnetization curves in the range to 60 kOe, the particle mean sizes in these samples were 3.8 and 4.6 nm in the 3h and 240h samples, respectively [33]. The Mössbauer technique was also used to characterize the samples. The processing of the Mössbauer spectra showed a good agreement with the parameters of the model spectra measured in ferrihydrite before [32, 33] and also showed that annealing of the samples did not lead to peculiarities indicating the formation of new phases of iron hydroxyl or oxide.

2.2. Measurements of Magnetic Properties

The quasi-static magnetic measurements were performed using a vibrating-coil magnetometer (VSM). The powder studied was fixed in paraffin in a measurement capsule. The temperature dependences of the magnetic moment M(H) were measured in the regimes of zero field cooling ZFC and the cooling in an external magnetic field (field cooling FC).

The magnetization curves M(H) were measured in pulsed magnetic fields on a unit at the Kirensky Institute of Physics of the Siberian Branch of RAS (Krasnoyarsk). A powder sample was reliably fixed in an inductive transducer of the pulse field magnetometer (PFM). The pulse duration (as the field changed from $H = 0 \rightarrow H_{max} \rightarrow H = 0$) was 16 ms. The magnetization isotherms were measured at various amplitudes of the magnetic field pulse up to 250 kOe. The data obtained using the PFM technique in the field range to 60 kOe well coincided with the results of the VSM measurements.

3. RESULTS AND DISCUSSION

Figure 1 shows the dependences of the magnetic moment $M(T)$ on the temperature of the samples measured in the ZFC and FC regimes. It is seen that dependences $M(T)_{ZFC}$ demonstrated the maxima corresponding to the SP blocking. The increase in the blocking temperature with an increase in the annealing time correlated to the increase in the sizes and, correspondingly, the mean magnetic moment of the particles $\langle\mu_P\rangle$ [32, 33, 36].

Figures 2 and 3 depict the experimental magnetization curves of the samples measured at various temperatures higher than the blocking temperature.[1] These figures contained the data measured in stationary (to 60 kOe) and pulse (to 250 kOe) fields. The measurements in pulsed fields were performed for each of the samples at two "edges" (the highest and the lowest) temperatures. We will make several remarks regarding to the measurements in pulsed fields. As is known, the blocking temperature of the SP particles is determined by the classical Néel– Brown relationship

$$T_B = KV/\ln(\tau/\tau_0)k_B, \quad (3)$$

where K is the magnetic anisotropy constant, V is the particle volume, k_B is the Boltzmann constant, and τ and τ_0 are the characteristic times of the measurement and relaxation of the particle ($\tau_0 \sim 10^{-9}$–10^{-11} s). In quasi-static magnetic measurements, a value $\tau \sim 10$–100 s was usually used [1], which led to relationship

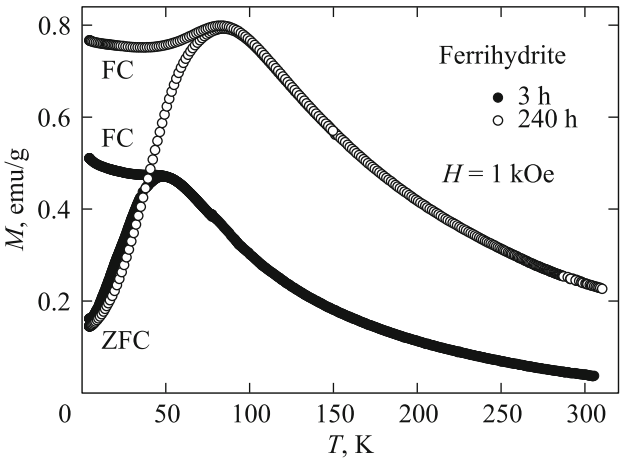

Fig. 1. Temperature dependences of magnetic moment $M(T)$ of ferrihydrite samples studied in the ZFC and FC regimes.

$T_B \approx KV/25k_B$. In the case of measurements in a pulsed field, the denominator of Eq. (3) was changed, which was observed, for example, as an increase in the coercive force of ε-Fe_2O_3 as the pulse period increased [38]. At $\tau \sim 8 \times 10^{-3}$ s (it is the time of increasing field to 250 kOe), T_B increased by a factor of ~1.3 as compared to quasi-static magnetic measurements. As a result, T_B ~48 and ~84 K (Fig. 1) will not be higher than the measurement temperature in pulsed magnetic fields (80 and 110 K for the 3h and 240h, respectively). The measurements at these temperatures by the PFM technique to 250 kOe observed a small hysteresis at the fields lower than 50 kOe, which was related to the relaxation processes of the particles with the highest blocking temperatures. In this field range (to 50–60 kOe), the experimental M(H) dependences were processed using the data obtained in stationary magnetic fields (VSM).

The solid curves in Figs. 2a and 3a illustrate the results of the best fitting of the dependences M(H) in the range of stationary fields to 60 kOe using Eq. (2) obtained in [33]. Actually, the adjustable parameters at a certain temperature were χ_{AF} and the mean magnetic moment of the particles $\langle\mu_P\rangle$ of the distribution function $f(\mu_P)$ that was the lognormal distribution

$$f(\mu_P) = (\mu_P s(2\pi)^{1/2})^{-1} \exp\{-[\ln(\mu_P/n)]^2/2s^2\},$$

where $\langle\mu_P\rangle = n\exp(s^2)$, s^2 is the dispersion of $\ln(\mu_P)$ that, as well as the number of particles N_P in Eq. (2), remained constant at various temperatures. The procedure described made it possible to describe the experimental data at a high accuracy to 60 kOe at various temperatures. Figures 2a and 3a also show the contributions (at indicated temperatures) corresponding to two terms of Eq. (2) and denoted as $f(\mu_P)$ and $\chi_{AF}H$. The large slope of the dependence $\chi_{AF}H$ (the second term) for the lower temperature reflects the

[1] Here and further in the text, the blocking temperature T_B was taken to be the temperature of the maximum of dependence $M(T)_{ZFC}$ (Fig. 1) that was proportional to the mean blocking temperature of the ensamble of SP particles [37] because of the existence of a distribution on the size and, therefore, on the values of T_B.

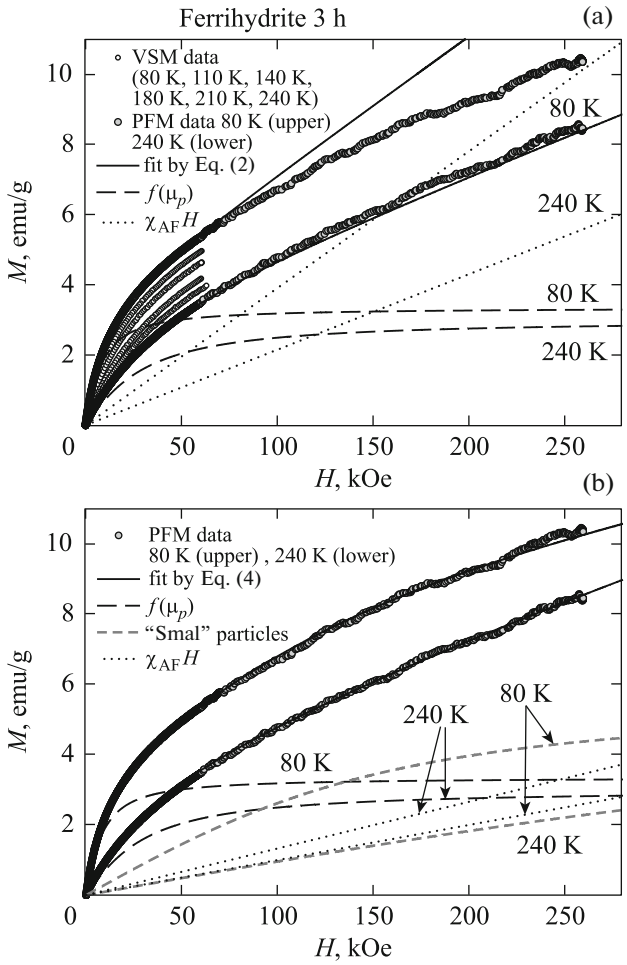

Fig. 2. Magnetization curves of ferrihydrite (3h sample) measured at various temperatures in various magnetic field ranges. The solid lines show the results of the best fitting of the data (a) for the range to 60 kOe by Eq. (2) and (b) for the range to 250 kOe by Eq. (4). The dashed and dotted lines show the contribution corresponding to the SP particles with the inclusion of the $f(\mu_P)$ distribution function, "small particles" (table), and also the contributions of the AF susceptibility $\chi_{AF}(H)$ at the noted temperatures.

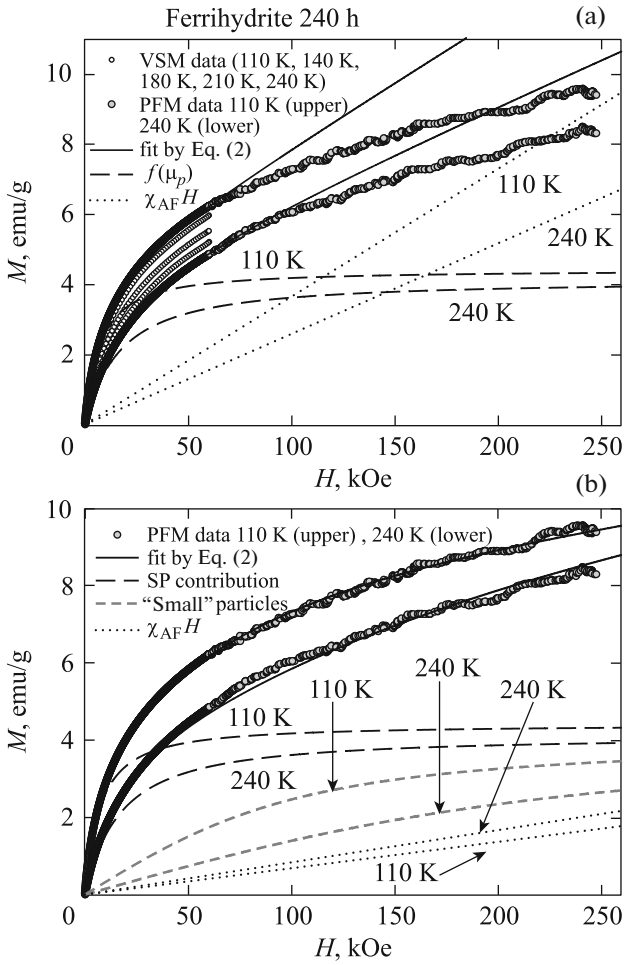

Fig. 3. Magnetization curves of ferrihydrite (240h sample) measured at various temperatures in various magnetic field ranges. The solid lines show the results of the best fitting of the data (a) for the range to 60 kOe by Eq. (2) and (b) for the range to 250 kOe by Eq. (4). The dashed and dotted lines show the contribution corresponding to the SP particles with the inclusion of the $f(\mu_P)$ distribution function, "small particles" (table), and also the contributions of the AF susceptibility $\chi_{AF}(H)$ at the noted temperatures.

"normal" behavior of the dependence $\chi_{AF}(T)$ discussed in Introduction.

At the same time, it is seen from Figs. 2a and 3a that there is a serious discrepancy between the experimental data and adjustable curves at high magnetic fields. The model curves showed were almost linear at high fields, which was due to the "saturation" of the Langevin function and the dominant influence of the second term in Eq. (2), while the experimental M(H) dependences had a negative curvature and did not attain the linear segment in fields to 250 kOe. Similar situation was observed in ferritin [4]: the slope of the experimental M(H) dependence (derivative dM/dH) became close to the calculated AF-susceptibility of ferritin only in fields of ~500 kOe. A linear increase in the M(H) dependence of ~25-nm NiO nanoparticles was observed in the field range 50–250 kOe [39]; i.e., $dM/dH \neq f(H)$ at $H > 50$ kOe.

Thus, we failed to attain the agreement between the experimental and model M(H) dependences of ferrihydrite over the entire field range by varying values of $\langle\mu_P\rangle$, χ_{AF}, and s^2 of distribution function $f(\mu_P)$ in the framework of the approach noted above (using Eq. (2)). And we hold to the idea that the observed character of the experimental M(H) dependences of the ferrihydrite samples, namely, that they did not achieve linear segments in the field range to 250 kOe, was due to the influence magnetic moments with low magnitude (small particles) which were not taken into account in the distribution function $f(\mu_P)$. In the other words, the M(H) dependence provided by the contribution of these small particles was a linear function of

Table 1. Parameters used upon fitting the experimental data (Figs. 2, 3) by Eqs. (2) ("coarse" particles) and (4) ("small" particles) and also particle sizes $\langle d \rangle$ and d_{SM} estimated using Eqs. (5) and (6), respectively

Sample	"Coarse" particles $f(\mu_P)$				"Small" particles			
	$\langle \mu_P \rangle$ $(T = 0)$	M_S $(T = 0)$ emu/g	N_P	$\langle d \rangle$, nm	μ_{SM}	M_{SM}, emu/g	N_{SM}	d_{SM}, nm
3 h	$320\mu_B$	3.45	1.61×10^{18}	3.8	$18\mu_B$	5.8	3.5×10^{19}	<1
240 h	$315\mu_B$	4.65	1.59×10^{18}	4.6	$40\mu_B$	5.1	1.4×10^{19}	~1

the external field in the range to ~50–60 kOe and had a characteristic "Langevin" bend with a tendency of flattening out to saturation only in higher magnetic fields. Then, the apparent decrease in the value of χ_{AF} with increase in temperature obtained as a result of fitting by Eqs. (1) or (2) was a result of the paraprocess characteristic of the SP contribution of these small magnetic moments.

We write the discussed contribution in the form $M_{SM}L(\mu_{SM}, H)$, where μ_{SM} is the magnetic moment, M_{SM} is the saturation magnetization related to the number of the particles N_{SM} in 1 g of the sample as follows: $M_{SM} = N_{SM}\mu_{SM}$.[2] Then, the magnetization curve will be described by the expression

$$M(H) = N_P \int_{\mu_{min}}^{\mu_{max}} L(\mu_P, H) f(\mu_P) \mu_P d\mu_P + M_{SM} L(\mu_{SM}, H) + \chi_{AF} H. \quad (4)$$

Figures 2b and 3b illustrate the results of the best fitting of the experimental data by Eq. (4) and the contributions of "coarse" $[f(\mu_P)]$ and "small' particles and the AF component $\chi_{AF}H$ corresponding to three terms of the right side of Eq. (4).

During the fitting procedure of the experimental data, the first term in Eq. (4) remained unchanged with respect to the results obtained before [33]; i.e., the contributions from the "coarse" particles with the distribution function $f(\mu_P)$ for the data shown in Figs. 2a and 2b and also 3a and 3b were the same. We varied only parameters M_{SM}, μ_{SM} (the same at various temperatures), and χ_{AF}. Table 1 gives the parameters obtained as a result of the aforementioned fitting procedure using Eq. (4). As is seen from Figs. 2b and 3b, the allowance for small magnetic moments allowed us to attain a good agreement between the fitting curves and the experimental M(H) dependences in fields to 250 kOe.

[2] In the M(H) dependence, we should take into account the quantization of a projection of small magnetic moment, which is performed by the Brillouin function. However, the difference between the Brillouin and the Langevin functions is insignificant for the obtained values of μ_{SM}, and the values of μ_{SM} obtained using these function is not larger than 10–15%, which does not influence the obtained results and the conclusions of this work.

Figure 4 illustrates the $\chi_{AF}(T)$ dependences obtained before from the processing of the M(H) dependences in the range to 60 kOe using Eq. (2) at various temperatures [33] and the data on the AF susceptibility obtained with the inclusion of the contribution of small magnetic moments by Eq. (4) when fitting the experiment to 250 kOe. The values of χ_{AF} obtained with the inclusion of the contribution of small particles were lower than the values obtained using Eq. (2); in addition, the values of χ_{AF} at low temperatures were low than those at high temperatures, which agreed with the classical behavior of the AF susceptibility of an antiferromagnet with a random orientation of the crystallographic axes at temperatures lower than the Néel temperature.

Actually, in the approach used, we used the bimodal magnetic moment distribution function of particles [40], which indicated the existence of two characteristic particle sizes. The size of the "coarse" particles can be obtained both immediately from the microscopy data and also by the indirect method, using the model concepts of the value of the noncompensated magnetic moment of an AF particle μ_P.

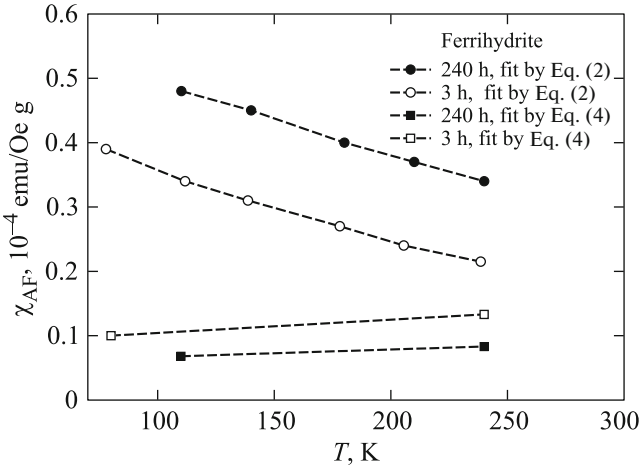

Fig. 4. AF susceptibility of ferrihydrite samples obtained by processing of the magnetization isotherms in fields to 60 kOe by Eq. (2) (Figs. 2a and 3a) and to 250 kOe by Eq. (4) (Figs. 2b and 3b).

According to Néel [41], the value of μ_P is determined by the relationship

$$\mu_P \sim JN^b, \quad (5)$$

in which N is the number of magnetoactive atoms in a particle, J is the atomic magnetic moment, and exponent b is dependent on the type of defects ($1/3 \le b \le 2/3$).

It can be assumed that $b \approx 1/2$ for ferrihydrite and ferritin [1, 15, 18–21, 23, 24, 26, and 42], which corresponded to a random disturbances of the magnetic order on the surface and in bulk of the particles. The values of $\langle d \rangle$ (table) obtained by the expression

$$\langle d \rangle \approx d_{\text{Fe–Fe}} N^{1/3} \approx d_{\text{Fe–Fe}} (\langle \mu_P \rangle / 5\mu_B)^{2/3}, \quad (6)$$

where $d_{\text{Fe–Fe}}$ is the mean distance between iron atoms in ferrihydrite ~0.31 nm [21] agrees well with data of transmission electron microscopy [33].

As for the "small" particles, which are difficult to be estimated immediately from the microscopic data, the number of iron atoms in these particles determined from Eq. (5) at $b \approx 1/2$ will be only ~10 (3 h sample) and 60 (240 h sample).[3] It is difficult to imagine a particle with such a small number of magnetically active atoms (in particular, for the first case), in which a magnetic order is retained. It is possible that b [Eq. (5)] takes a smaller value for extremely small particles, and similar hypothesis was proposed in [43]. However, in any case, the magnetic moments of 15–$40\mu_B$ were most likely provided either by ~1-nm ferrihydrite particles or disordered complexes of iron, oxygen, and carbon atoms [31, 44, 45]. During a prolonged annealing (240h sample), these complexes can form ferrihydrite particles, and, as is seen from the table, the number of the "small" particles decreased after annealing and their sizes increased, since their magnetic moment increased. The similar scenario of increasing the particle sizes as a result of annealing, namely, the agglomeration of the nearby particles, follows from an analysis of the results of the study of annealed ferrihydrite [24, 32–34].

These estimations of the "small" particle sizes had a very qualitative character, but the presence of a significant magnetic contribution provided by these small particles was observed in a nonlinear dependence M(H) in high fields. Based on the analysis performed above, we can speak about a bimodal type of the particle size distribution, at least, in the bacterial ferrihydrite under study. The agreement between the experimental data on magnetization in high fields obtained in this work and the results of [4], in which ferritin was studied, indicated, possibly, the general features of the character of the size distribution of magnetic moments of particles in bioferrihydrite and ferritin. In addition, the inclusion of the SP behavior of the small particles made it possible to conclude that the $\chi_{AF}(T)$ dependence for ferrihydrite was a function that increased with temperature, which was typically for an antiferromagnet with random orientation of the crystallographic axes, according to the conclusions of [4].

[3] For the "small" particles, there is the distribution function with respect to magnetic moments and sizes; however, the processing of the experimental results taking into account the distribution function led to similar results, i.e., $\mu_{SM} \approx \langle \mu_{SM} \rangle$, but, in this case, the number of adjustable parameters was increased.

4. CONCLUSIONS

In this work, we studied the processes of magnetization of nanoparticles of the antiferromagnetically ordered ferrihydrite of various sizes in strong (to 250 kOe) magnetic fields. According to the commonly accepted approach of the AF nanoparticles, the magnetization curve is a superposition of the contributions from the noncompensated magnetic moments of the particles and the antiferromagnetically ordered "core." However, the determination of the AF contribution, i.e., numerical values of the AF susceptibility χ_{AF} and also its temperature dependence was dependent on a magnetic field range used when analyzing the experimental data. In the case of commonly accepted magnetic fields to 60 kOe (the range was determined by the standardization of the installations), the $\chi_{AF}(T)$ dependence was a function decreasing with the increase in temperature, and the analysis of the M(H) dependences in the fields to 250 kOe showed that the $\chi_{AF}(T)$ dependence was a function that increased with temperature. The latter agrees with the behavior of a system of AF particles with a random orientation of the crystallographic axes at temperatures lower than the Néel temperature. The observed crossover introduced serious corrections to the physical interpretation of the experimental curves of magnetization of nanoparticles of ferrihydrite or ferritin: the decrease in the value of χ_{AF} with the increase in temperature observed by many authors was not related to the superantiferromagnetism effect and was most likely induced by the influence of low magnetic moments that can be simply taken into account by substantial expansion of the range of used magnetic fields.

ACKNOWLEDGMENTS

This work was supported by the Russian Foundation for Basic Research, the Government of Krasnoyarsk region, the Krasnoyarsk Regional Foundation of Supporting the Scientific and Scientific–Engineering Activity in the framework of the scientific projects nos. 17-42-240138 and 17-43-240527.

REFERENCES

1. S. Mørup, D. E. Madsen, C. Fradsen, C. R. H. Bahl, and M. F. Hansen, J. Phys.: Condens. Matter **19**, 213202 (2007).
2. D. E. Madsen, S. Mørup, and M. F. Hansen, J. Magn. Magn. Mater. **305**, 95 (2006).

3. Yu. L. Raikher and V. I. Stepanov, J. Phys.: Condens. Matter. **20**, 204120 (2008).
4. N. J. O. Silva, A. Millan, F. Palacio, E. Kampert, U. Zeitler, and V. S. Amaral, Phys. Rev. B **79**, 104405 (2009).
5. Yu. L. Raikher and V. I. Stepanov, J. Exp. Theor. Phys. **107**, 435 (2008).
6. Yu. L. Raikher, V. I. Stepanov, S. V. Stolyar, V. P. Ladygina, D. A. Balaev, L. A. Ishchenko, and M. Balasoiu, Phys. Solid State **52**, 298 (2010).
7. A. Punnoose, H. Magnone, M. S. Seehra, and J. Bonevich, Phys. Rev. B **64**, 174420 (2001).
8. S. D. Tiwari and K. P. Rajeev, Solid State Commun. **152**, 1080 (2012).
9. S. A. Makhlouf, H. Al-Attar, and R. H. Kodama, Solid State Commun. **145**, 1 (2008).
10. A. Punnoose and M. S. Seehra, J. Appl. Phys. **91**, 7766 (2002).
11. A. A. Lepeshev, I. V. Karpov, A. V. Ushakov, D. A. Balaev, A. A. Krasikov, A. A. Dubrovskiy, D. A. Velikanov, and M. I. Petrov, J. Supercond. Nov. Magn. **30**, 931 (2017).
12. R. H. Kodama and A. E. Berkowitz, Phys. Rev. B **59**, 6321 (1999).
13. S. Giri, M. Patra, and S. Majumdar, J. Phys.: Condens. Matter **23**, 073201 (2011).
14. A. A. Dubrovskiy, D. A. Balaev, K. A. Shaykhutdinov, O. A. Bayukov, O. N. Pletnev, S. S. Yakushkin, G. M. Bukhtiyarova, and O. N. Martyanov, J. Appl. Phys. **118**, 213901 (2015).
15. C. Gilles, P. Bonville, H. Rakoto, J. M. Broto, K. K. W. Wong, and S. Mann, J. Magn. Magn. Mater. **241**, 430 (2002).
16. D. A. Balaev, A. A. Dubrovskiy, K. A. Shaykhutdinov, O. A. Bayukov, S. S. Yakushkin, G. A. Bukhtiyarova, and O. N. Martyanov, J. Appl. Phys. **114**, 163911 (2013).
17. M. J. Martínez-Pérez, R. de Miguel, C. Carbonera, M. Martínez-Júlvez, A. Lostao, C. Piquer, C. Gómez-Moreno, J. Bartolomé, and F. Luis, Nanotechnology **21**, 465707 (2010).
18. N. J. O. Silva, V. S. Amaral, and L. D. Carlos, Phys. Rev. B **71**, 184408 (2005).
19. D. A. Balaev, A. A. Dubrovskii, A. A. Krasikov, S. V. Stolyar, R. S. Iskhakov, V. P. Ladygina, and E. D. Khilazheva, JETP Lett. **98**, 139 (2013).
20. S. A. Makhlouf, F. T. Parker, and A. E. Berkowitz, Phys. Rev. B **55**, R14717 (1997).
21. A. Punnoose, T. Phanthavady, M. S. Seehra, N. Shah, and G. P. Huffman, Phys. Rev. B **69**, 054425 (2004).
22. M. S. Seehra, V. Singh, X. Song, S. Bali, and E. M. Eyring, J. Phys. Chem. Solids **71**, 1362 (2010).
23. C. Gilles, P. Bonville, K. K. W. Wong, and S. Mann, Eur. Phys. J. B **17**, 417 (2000).
24. D. A. Balaev, A. A. Krasikov, A. A. Dubrovskii, S. V. Semenov, O. A. Bayukov, S. V. Stolyar, R. S. Iskhakov, V. P. Ladygina, and L. A. Ishchenko, J. Exp. Theor. Phys. **119**, 479 (2014).
25. Chandni Rani and S. D. Tiwari, J. Magn. Magn. Mater. **385**, 272 (2015).
26. M. S. Seehra, V. S. Babu, A. Manivannan, and J. W. Lynn, Phys. Rev. B **61**, 3513 (2000).
27. S. V. Stolyar, R. N. Yaroslavtsev, R. S. Iskhakov, O. A. Bayukov, D. A. Balaev, A. A. Dubrovskii, A. A. Krasikov, V. P. Ladygina, A. M. Vorotynov, and M. N. Volochaev, Phys. Solid State **59**, 555 (2017).
28. L. Néel, C.R. Acad. Sci. Paris **253**, 1286 (1961).
29. L. Néel, C.R. Acad. Sci. Paris **253**, 203 (1961).
30. Ch. Rani and S. D. Tiwari, Physica B **513**, 58 (2017).
31. S. V. Stolyar, O. A. Bayukov, Yu. L. Gurevich, V. P. Ladygina, R. S. Iskhakov, and P. P. Pustoshilov, Inorg. Mater. **43**, 638 (2007).
32. D. A. Balaev, A. A. Krasikov, A. A. Dubrovskii, O. A. Bayukov, S. V. Stolyar, R. S. Iskhakov, V. P. Ladygina, and R. N. Yaroslavtsev, Tech. Phys. Lett. **41**, 705 (2015).
33. D. A. Balaev, A. A. Krasikov, A. A. Dubrovskiy, S. I. Popkov, S. V. Stolyar, O. A. Bayukov, R. S. Iskhakov, V. P. Ladygina, and R. N. Yaroslavtsev, J. Magn. Magn. Mater. **410**, 71 (2016).
34. D. A. Balaev, A. A. Krasikov, A. A. Dubrovskiy, S. V. Semenov, S. I. Popkov, S. V. Stolyar, R. S. Iskhakov, V. P. Ladygina, and R. N. Yaroslavtsev, Phys. Solid State **58**, 287 (2016).
35. D. A. Balaev, A. A. Krasikov, A. A. Dubrovskiy, S. I. Popkov, S. V. Stolyar, R. S. Iskhakov, V. P. Ladygina, and R. N. Yaroslavtsev, J. Appl. Phys. **120**, 183903 (2016).
36. D. A. Balaev, A. A. Krasikov, S. V. Stolyar, R. S. Iskhakov, V. P. Ladygina, R. N. Yaroslavtsev, O. A. Bayukov, A. M. Vorotynov, M. N. Volochaev, and A. A. Dubrovskii, Phys. Solid State **58**, 1782 (2016).
37. J. C. Denardin, A. L. Brandl, M. Knobel, P. Panissod, A. B. Pakhomov, H. Liu, and X. X. Zhang, Phys. Rev. B **65**, 064422 (2002).
38. D. A. Balaev, I. S. Poperechny, A. A. Krasikov, K. A. Shaikhutdinov, A. A. Dubrovskiy, S. I. Popkov, A. D. Balaev, S. S. Yakushkin, G. A. Bukhtiyarova, O. N. Martyanov, and Yu. L. Raikher, J. Appl. Phys. **117**, 063908 (2015).
39. D. A. Balaev, A. A. Dubrovskii, A. A. Krasikov, S. I. Popkov, A. D. Balaev, K. A. Shaikhutdinov, V. L. Kirillov, and O. N. Mart'yanov, Phys. Solid State **59** (2017), in press.
40. B. P. Khrustalev, A. D. Balaev, and V. M. Sosnin, Phys. Solid State **37**, 911 (1995).
41. L. Néel, C.R. Acad. Sci. Paris **252**, 4075 (1961).
42. J. G. E. Harris, J. E. Grimaldi, D. D. Awschalom, A. Chiolero, and D. Loss, Phys. Rev. B **60**, 3453 (1999).
43. T. H. Lee, K.-Y. Choi, G.-H. Kim, B. J. Suh, and Z. H. Jang, Phys. Rev. B **90**, 184411 (2014).
44. M. Balasoiu, S. V. Stolyar, R. S. Iskhakov, L. A. Ischenko, Y. L. Raikher, A. I. Kuklin, O. L. Orelovich, Yu. S. Kovalev, and T. S. Kurkin, Roman. J. Phys. **55**, 782 (2010).
45. S. V. Stolyar, O. A. Bayukov, V. P. Ladygina, R. S. Iskhakov, L. A. Ishchenko, V. Yu. Yakovchuk, K. G. Dobretsov, A. I. Pozdnyakov, and O. E. Piksina, Phys. Solid State **53**, 100 (2011).

Translated by Yu. Ryzhkov